



The value of DTI: achieving high diagnostic performance for brain metastasis

Ma Liheng¹ · Xu Guofan² · Rosario Francesco Balzano³ · Liang Yuying¹ · Hong Weifeng¹ · Yang Ning⁴ · Ji Yayun¹ · Liu Mouyuan¹ · Giuseppe Guglielmi³

Received: 1 December 2019 / Accepted: 8 June 2020 / Published online: 20 June 2020
© Italian Society of Medical Radiology 2020

Abstract

Background The evaluation of brain metastases generally requires post-contrast MRI exam, but some patients have contraindication to contrast medium administration.

Purpose To investigate the value of the MRI diffusion tensor imaging (DTI) for detection of metastatic brain tumor.

Materials and methods We retrospectively analyzed the MRI data from 23 patients (13 males and 10 females) with brain metastases. The MRI protocol consisted in T1WI, T2WI, post-contrast 3DT1WI and DTI images ($b = 1000$) sequences. The brain metastatic lesions were counted in each of these sequences. We compared the advantages and limitations of different sequences in the brain metastases detection. The number of metastatic lesions identified on the contrast-enhanced 3DT1WI image is used as the reference. FA values were measured in the intratumoral, adjacent peritumoral and distant peritumoral edema area (PTEA) of brain metastasis, and the differences were statistically analyzed.

Results DTI can detect more brain metastatic lesions rather than T1WI and T2WI. The number of brain metastases on DTI is similar to post-contrast 3D T1WI. There is no statistical difference in the FA value change between the adjacent and distant PTEA.

Conclusion The DTI original image can be used as an alternative examination for patients with contraindications to contrast-enhanced MRI. It has high sensitivity to intratumoral hemorrhage, which has advantage to detect brain metastatic lesions as compared with T1WI or T2WI images.

Keywords Brain metastases · Magnetic resonance imaging (MRI) · Diffusion tensor imaging (DTI) · Post-contrast Imaging

Introduction

Metastatic brain tumor is the most common malignant tumor of the central nervous system in adults. Brain metastases usually suggest poor prognosis; hence, early detection and accurate identification are of great significance for tumor staging, clinical management and therapeutic schedule, which may lead to improved prognosis [1, 2]. MRI is currently the best choice for detection of metastatic brain tumors [3–5]. Contrast-enhanced MR imaging is commonly used in clinical practice to identify small lesions, especially without peritumoral edema, which usually could not be detected with conventional non-contrast MRI images such as T1WI or T2WI. Some Authors have proposed to use a double dose of contrast medium to improve the detection rate of lesions [6, 7]. However, some patients cannot undergo contrast-enhanced MRI because of the contrast agents allergy or renal insufficiency. Furthermore, nephrogenic systemic fibrosis

✉ Giuseppe Guglielmi
giuseppe.guglielmi@unifg.it

¹ Imaging Department, First Affiliated Hospital of Guangdong Pharmaceutical University, Guangzhou City, Guangdong Province, China

² Division of Diagnostic Imaging, Department of Nuclear Medicine and Imaging Physics, MD Anderson Cancer Center, Houston City, TX, USA

³ Department of Clinical and Experimental Medicine, University School of Medicine, Viale L. Pinto, 1, 71121 Foggia, Italy

⁴ Pathology Department, First Affiliated Hospital of Guangdong Pharmaceutical University, Guangzhou City, Guangdong Province, China

caused by MRI contrast medium has attracted increasing attention. Therefore, it is essential for us to explore the diagnostic value of other non-contrast magnetic resonance imaging sequences in detection of metastatic brain tumors and to find a feasible alternative for the patients with contraindications to contrast agent injection. Compared to DWI sequences, DTI sequences exert more gradient fields in many directions which results in growingly sensitive to the movement of water molecules. Except for reflecting the diffusion movement of water molecules, DTI sequences can also provide further information. Previous studies have focused on the application of DTI tractography to quantifying the white matter fiber of brain tumors [8–12].

To the best of our knowledge, there is no prior report about using the DTI to detect the metastatic brain tumor. The aim of this study is to evaluate DTI for the detection of brain metastases in comparison with post-contrast 3D T1WI. This may give us an alternative MRI protocol for the patients who have suspicious brain metastases but contraindications to the MRI contrast.

Materials and methods

Subjects

This population-based cohort study of adult patients was retrospectively assessed based on the data from our hospital. As approved by our hospital IRB Ethics Committee for this retrospective imaging analysis, the informed consents were waived. Between July 2017 and October 2018, a total of 23 patients with multiple brain metastases were included in this study. Patients underwent brain MRI examination with morphological, post-contrast 3D T1 and DTI acquisitions. Patients with a solitary brain metastasis were excluded. Patients' mean (SD) age was 58.20 (9.21) years. Among them, there were 13 males with the median age of 59 and 10 females with the median age of 54 years. The primary tumors of these cases include 19 lung cancer (1 case of small cell carcinoma and 18 cases of adenocarcinoma), 1 case of invasive cervical carcinoma, 1 case of hepatocellular carcinoma, 1 case of breast cancer and 1 case of rectal cancer. The primary tumors of all patients involved in this study were confirmed for about 6 months to 5 years prior to the MRI brain exam. All these patients were diagnosed with multiple brain metastases during the treatment of the primary malignant tumor. The therapeutic regimen of the primary tumor includes chemotherapy, chemoradiotherapy, biotherapy and/or surgery.

Imaging protocol

Patients with suspected metastatic brain tumor underwent brain MRI examination (3.0T MRI, General Electric Company, 750 W), with the standard quadrature transmit and receive head coil with 16-rung structure, and contrast medium was also administered. The MRI sequences included T1-weighted images (T1WI) (TR/TE: 488/15 ms) T2-weighted images (T2WI) (TR/TE: 3800/100 ms) and coronal T2-FLAIR (TR/TE:3800/100 ms; TI:2000 ms), contrast-enhanced 3D T1WI sequence (3D BRAVO). All sequences were acquired with the following parameters: FOV 240 × 240 mm, matrix: 320 × 256 mm; slice thickness/space: 5 mm/1 mm (1 mm without gap in the 3D BRAVO), number of excitation: 2 to 3. The DTI was performed by single-shot spin echo–echo-planar imaging; the parameters were: TR/TE: 8000/98.6 ms, 2 mm slice thickness with no gap, 15–20 directions, *b* value was 0 and 1000 s, FOV: 240 × 240 mm, matrix: 112 × 111 mm. The imaging time was 5 min 36 s–5 min 44 s. The contrast agents were gadopentetate dimeglumine (Magnevist, Bayer, 0.2 ml/kg body weight, 1–2 ml/s) by i.v injection with powered pressure syringe via the vein at antecubital fossa (Magnevist is still used to be the routine contrast medium during MRI in China; there is no associated prohibition about its use).

Image Analysis

All data were transferred to the radiology PACS workstation. Two neuroradiologists with 27 and 17 years of experiences, respectively, reviewed the brain MR images, and the agreements were reached with consensus. The imaging features include the location of the lesion, morphology, signal and enhancement characteristics on each sequence. The number of metastases was counted on each sequence. In 7 patients, fractional anisotropy (FA) values of 13 brain metastases with obvious peritumoral edema were measured from the “no necrotic area within the tumor,” “adjacent peritumoral edema” (area within 1 cm of peritumoral edema) and “distant peritumoral edema” (area outside 1 cm of peritumoral edema) (Fig. 1). The rate of FA value change within the tumor and in the adjacent and distant area of peritumoral edema was calculated separately. The rate of FA value change was defined as:

The change rate of FA value = (FA value measured in the contralateral healthy side – FA value of the affected side)/FA value measured in the contralateral hemisphere to the lesion side [13, 14]. The ROI of the contralateral healthy side was the copy of the affected side symmetrically (Fig. 1).

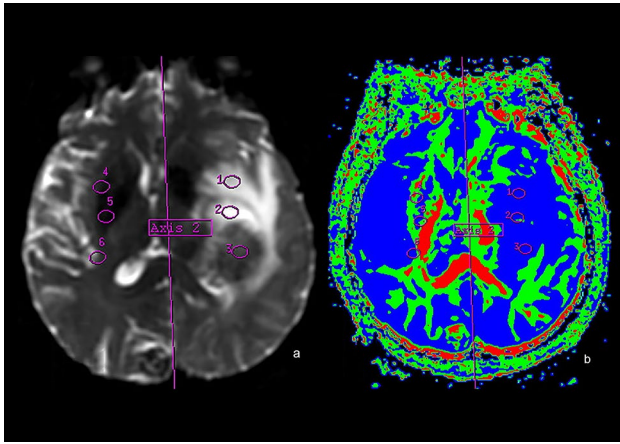


Fig. 1 Example of ROI analysis measurements of brain metastases. **a** $b=0$ DWI, **b** FA image. 1: measurement of the ROI of the distant peritumoral edema (area outside 1 cm from the outer edge of tumor), 2: measurement of the ROI of the adjacent peritumoral edema (area within the 1 cm from the outer edge of tumor), 3: measurement of the ROI within the tumor. 4, 5, 6: measurement of ROIs in the contralateral normal brain tissue

The area of interest is about $0.5\text{--}1.3\text{ cm}^2$. To decrease the sampling bias, repeated measurements were taken for three times within a month and the mean value was calculated for analysis.

IBM SPSS Statistical Software (version 22.0, IBM Corp, Armonk, NY, 2013) was used for all analysis. Bivariate correlation analysis was performed on the number of lesions detected in 23 patients, between plain T1WI, T2WI, DTI and 3D post-contrast T1WI [15]. Three sets of correlation coefficients were calculated. The counting results of 3DT1WI contrast-enhanced sequence were taken as dependent variables, and the counting results of T1WI, T2WI and DTI were taken as independent variables for simple linear regression and to calculate the determination coefficient R-squared. Cordon R language compiled

by Deisenhofer et al. [15] was used to compare the correlation coefficients of T1WI/3DT1WI contrast enhancement, T2WI/3DT1WI contrast enhancement and DTI/3DT1WI contrast enhancement, respectively, and moreover, statistically analyze the consistency of the results of DTI and 3DT1WI contrast enhancement combining the results of the coefficient R-squared.

A *t* test of two independent samples was used to compare the difference of FA value change rate between adjacent and distant peritumoral edema, and $P < 0.05$ was considered statistically significant. Because the FA value measurements of the intratumoral solid components demonstrated great variation, the further statistical analysis was not performed.

Results

The manifestation of metastatic brain tumor on conventional MRI

All the patients included in the current study have multiple brain lesions. Most of the brain metastases show a T1 iso-/hypo-intensity and a T2 iso- or slightly hyper-intensity. Punctate or patchy hemorrhage can be seen in the lesions, which presents as high signal on T1WI and low signal on T2WI. When there is tumor necrosis, high T2 signal can be seen on T2WI. Based on the enhancement characteristics of the lesion, three patterns can be distinguished:

1. uniform or non-uniform enhancement of the entire tumor (Figs. 2, 3),
2. rim enhancement with central or eccentric necrosis and nodular enhancement (Figs. 4, 5),
3. circular or irregular ring enhancement without necrotic center (Fig. 6).

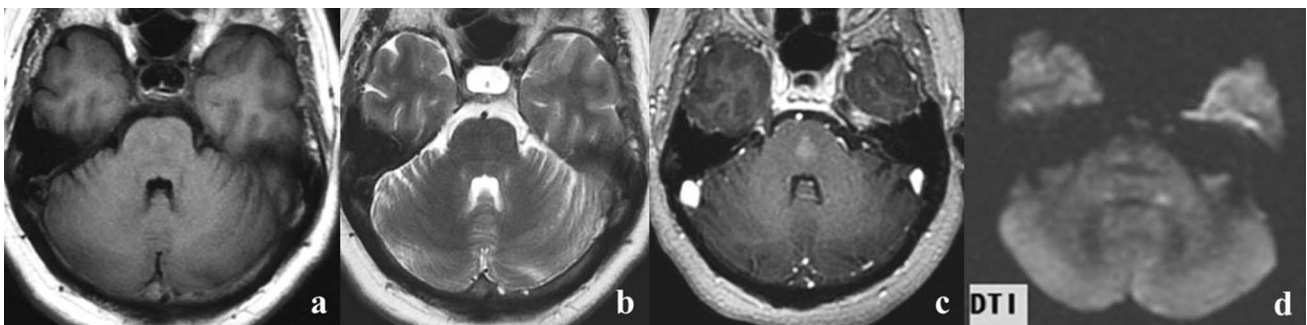


Fig. 2 Small pontine metastasis. **a** axial T1WI, **b** axial T2WI, **c** axial post-contrast 3D T1WI, **d** axial DTI. The lesion is barely visible on T1 and T2 wi and experts a modest CE on post-contrast T1wi. On

DTI, the lesion is hardly recognizable as focal hypo-intensity surrounded by a slight area of peripheral edema

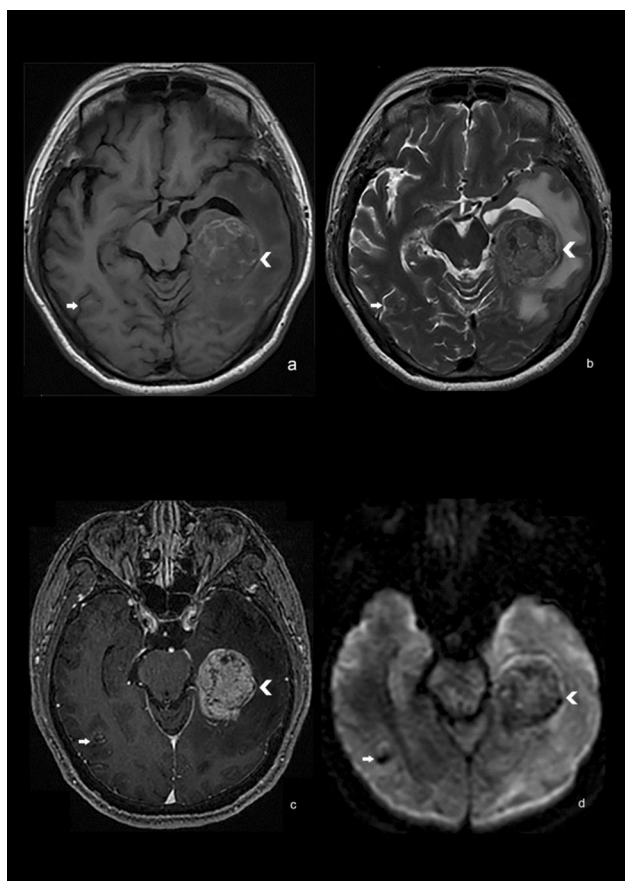


Fig. 3 62-year-old female with lung adenocarcinoma metastasis. **a** axial T1WI, **b** axial T2WI, **c** axial post-contrast 3D T1WI, **d** axial DTI. A large round-like metastasis is observed in the right temporal lobe (arrow head); a smaller lesion (arrow) is also seen in the right temporal lobe. **a, b** The bigger lesion appears iso- or mild hypo-intense on T1WI and iso-intense on T2WI. The intratumoral hemorrhage has high signal intensity on T1WI and low signal intensity on T2WI. The smaller lesion in the right temporal lobe shows faintly on the T1WI and T2WI, with iso- and mild hypo-intensity signal on both T1WI and T2WI. A rim of low signal intensity is also seen around the smaller lesion on the T2WI. **c** On post-contrast 3D T1WI sequence, the lesion in the left temporal lobe undergoes remarkably enhancement with few punctured and patchy low-signal areas without enhancement, corresponding to the low-signal areas on T2WI. The lesion of the right temporal lobe presented spotty enhancement. **d** On DTI, the smaller lesion is clearly outlined. Both lesions were well defined and their extension is larger than the conventional T1WI and T2WI. The extent of the intratumoral hypo-intensity is also larger than the conventional T2WI. The peritumoral edema in the left temporal lobe has a slightly high signal intensity on the DTI

There is usually no enhancement of the hemorrhage area in the lesion.

The imaging feature of brain metastases on the DTI

Hemorrhagic lesions with high signal on T1WI and low signal on T2WI showed low signal intensity on the DTI

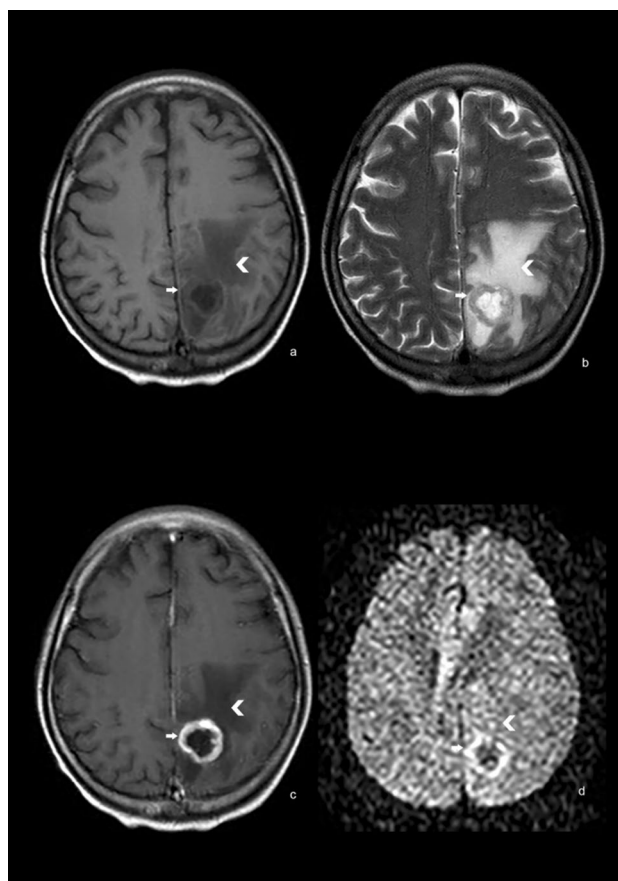


Fig. 4 A 50-year-old woman with brain metastases cervical cancer. **a** Axial T1WI, **b** axial T2WI, **c** post-contrast axial 3D T1WI, **d** axial DTI. **a, b** The lesion shows irregular thick-walled nodules with necrotic cystic changes. The wall shows iso-intensity on both T1WI and T2WI (arrow), and extensive perilesional edema (arrow head) is also present. **c** On post-contrast 3D T1WI, the wall undergoes intense enhancement (arrow), while the peritumoral edema is still hypo-intense (arrow head). **d** On DTI, the necrotic area within the tumor has low signal intensity, while the tumor wall (arrow) has a high signal. The signal intensity of peritumoral edema (arrow head) is slightly higher than the normal contralateral white matter

sequence. Compare to the conventional T1WI and T2WI, the extent of the low signal of some lesions was much more remarkable on the DTI, and the number of the lesions with low signal intensity on the DTI was greater than those identified on the conventional T1W and T2W images.

Peritumoral edema shows slightly high signal on the DTI. Enhanced tumor parenchyma showed slightly high signal or high signal on the DTI (Figs. 3, 6).

The cystic portion of the lesion usually showed low signal intensity on the DTI, while some lesions showed slightly high signal intensity. The cystic wall showed a high signal on the DTI (Fig. 4), which is also expected to show contrast enhancement on the post-contrast T1WI images. The central nodule and the enhancing part of the metastatic lesion showed a high signal on the DTI (Fig. 5).

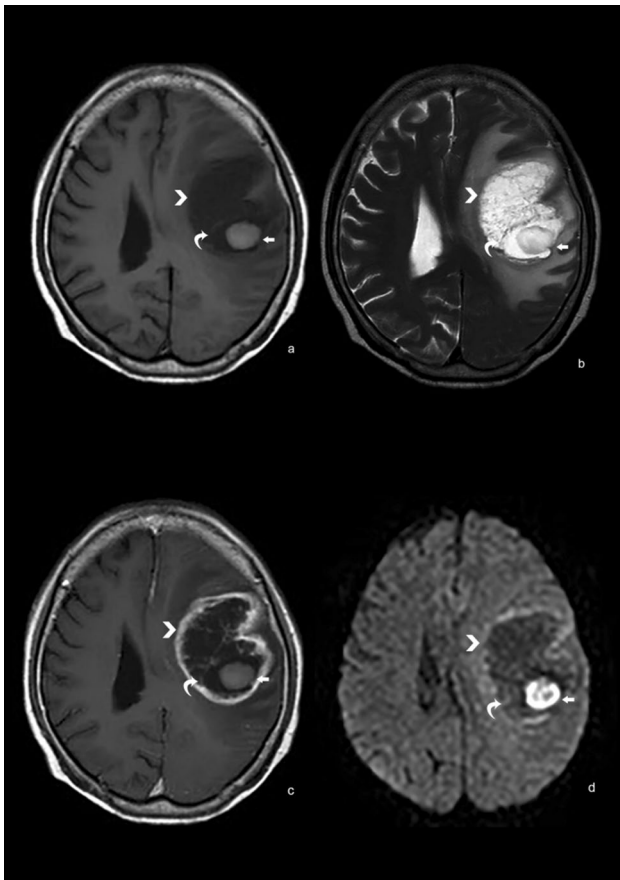


Fig. 5 A 77-year-old woman with rectal cancer and brain metastasis. **a** axial T1WI, **b** axial T2WI, **c** contrast-enhanced axial 3D T1WI, **d** axial DTI. **a, b** An irregular cystic lesion (arrow head) with low signal on T1WI and high signal on T2WI was observed in the left frontal lobe. There were multiple fine septum (curved arrow) within the tumor, which appeared iso-intensity on T1WI and slightly hypo-intensity on T2WI. A wall nodule (straight arrow) with high signal intensity on T1WI and slightly high signal intensity on T2WI is appreciated on the left posterior wall of the metastatic tumor (straight arrow). **c** On post-contrast 3D T1WI, the tumor shows irregular ring shaped (arrow head) and wall nodule enhancement, while the internal septum undergoes mild enhancement. **d** On DTI, the enhanced tumor wall and wall nodule (straight arrow) show visible high signal intensity

Comparison of lesions count on each sequence

A total of 123 lesions were found on T1WI, 130 lesions on T2WI, 185 lesions on 3DT1WI (range size 5–237 mm in diameter) and 167 lesions on DTI (range size 7–237 mm in diameter). DTI detection of small lesions located below the inner plate of the skull bone and on the brain gyri was lower than the 3DT1WI. Referring to the 3DT1WI as the golden standard, the percentages of detection of lesions on T1WI were 123/185 (66.5%), on T2WI was 130/185 (70.3%) and on DTI was 167/185 (90.3%). These results suggest that the lesion count on DTI is more consistent with the post-contrast

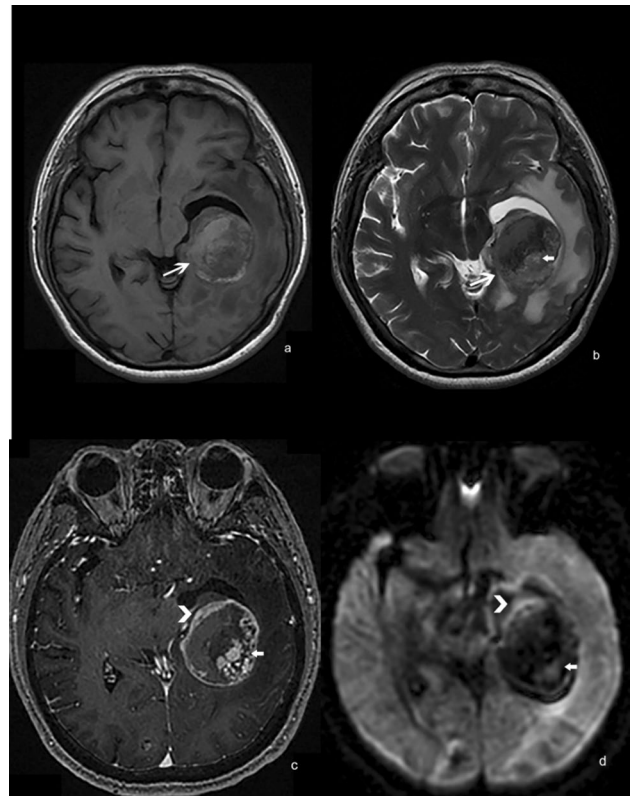


Fig. 6 A 55-year-old man with brain metastasis from lung adenocarcinoma. **a** Axial T1WI, **b** axial T2WI, **c** contrast-enhanced axial 3D T1WI, **d** Axial DTI. **a, b** A round-like lesion (long arrow) with iso- or mild hypo-intensity on T1WI and iso-intensity on T2WI is observed in the deep left temporal lobe. The intratumoral hemorrhage has high signal intensity on T1WI and low signal intensity on T2WI. There were patchy slightly high signal intensities (short arrow) within the left posterior of the lesion. **c** On post-contrast 3D T1WI, the wall lesion undergoes intense CE (arrow head) and some nodules (arrow) can be also appreciated in the left posterior portion. **d** The DTI shows high signal intensity in the corresponding T2 hypo-intensity. The enhancing portion on the post-contrast 3D T1WI sequence appears as mild high signal intensity areas (arrow and arrow head)

3DT1WI compared to the T1WI or T2WI sequences. The number of lesions in the 3DT1WI contrast enhancement images was taken as the dependent variable, and the number of lesions in the T1WI/T2WI/DTI was taken as the independent variable, the determination coefficients R^2 obtained were 0.916, 0.914 and 0.975, respectively. Among the correlation coefficients, the DTI shows highest consistency compared to the contrast enhance 3DT1WI.

Peritumoral edema

The degree of peritumoral edema varies. Some small lesions appeared remarkable edema, whereas some large lesions only present with minimal edema (Figs. 3, 4). The peritumoral edema was mainly located in the gray-white junction

of the frontal, temporal and parietal lobe and adjacent to the venous sinus.

FA value measurements of the intratumoral solid components demonstrated great variation, with some lesions showing high FA values and others have low values. Such large variation might be due to intratumoral hemorrhage. The intratumoral FA change rate comparison was not conducted due to such high variations.

The *T* test results of two independent samples about the change rate of FA value in the adjacent and distant peritumoral edema showed that the change rate of FA value was 0.40 ± 0.12 , 0.44 ± 0.12 , respectively. There was no statistically significant difference in the change rate of FA value between the adjacent and distant peritumoral edema by the *t* test of two independent samples statistic analysis ($t = -0.677$, $P = 0.505 > 0.05$, homogeneity of variance test, $F = 0.201$, $P = 0.658$).

Discussion

When brain metastases occur in primary malignant tumors, the prognosis becomes poor. Early detection and accurate determination of the number of brain metastases are of great importance for tumor staging, treatment planning and prognosis [1, 3]. Brain metastatic tumors not only break the blood–brain barrier, but also have rich neoplastic neovascularization, which commonly leads to bleeding, necrosis and cystic changes. Nodular, annular or irregular enhancement is the common imaging features. The contrast-enhanced MRI scan is considered to be the gold for the diagnosis of brain metastases [16, 17] for its greater sensitivity and specificity in the detection of small intracranial lesions as compared to MRI brain exam without contrast [18, 19].

Some authors have suggested a double-dose contrast enhancement MRI protocol for the evaluation of brain metastases; also new contrast agents were recently developed to improve the detection rate [20–22].

In clinical practice, the use of contrast-enhanced MRI sometimes is limited due to the gadolinium contrast allergy and its risk for nephrogenous systemic fibrosis.

With the recent high-field MRI scanner improvements, several studies tried to use many functional sequences to detect brain metastases earlier and more accurately [23, 24]. This study aimed to provide a supplementary or alternative examination scheme for patients with contraindications of gadolinium-based MRI contrast.

Diffusion tensor imaging (DTI) is an advanced MR imaging technique that makes use of diffusion-weighted imaging principles. A typical DTI dataset contains at least one base image and six or more diffusion-weighted images obtained along noncollinear encoding directions. Compared with classical DWI, DTI exerts gradient fields along each

direction at a time and are more sensitive to the movement of water molecules. In fact, DTI can also provide more information regarding the histological structure of the brain, i.e., the structure of the white matter fiber tract [25–27]. FA value is a parameter, which is based on the weighted values of the necessary images and the three principal axes of diffusion-weighted imaging and diffusion tensor obtained in six or more directions. FA value reflects the diffusivity tendency of water molecules along the white matter fiber bundles. $FA = 0$ represents isotropic diffusion, $FA = 1$ represents 100% specificity along the direction of the maximum eigenvector and is anisotropic diffusion. In general, the anisotropic fraction of tumors is lower than that of normal white matter, due to the destruction of standard nerve fibers and the proliferation of tumor cells leading to a reduced diffusion direction. Recently, Bette S. and colleagues showed that FA may be useful for the differentiation between brain metastases and CNS lymphoma [28].

Among the 23 patients included in this study, lung cancer accounted for 19/23. Histologically, lung cancer metastases tend to bleed because the tumor blood vessels are prone to rupture due to the intravascular hypertension which is secondary of tumor cells infiltration, increased vascular permeability and intravascular thrombosis [29–32]. Moreover, all patients were diagnosed with brain metastases during history of the primary malignant tumor. Treatment regime of the primary tumor may also result in bleeding within the metastatic tumor, which is consistent with the imaging manifestations of bleeding signals on magnetic resonance sequences. On DTI, the tumorous architecture containing bleeding components appeared low signal intensity, and the area of the low signal is larger than the T2WI image, suggesting the blood-related susceptibility artifact. Echo-planar imaging (EPI) is commonly used in the diffusion-weighted imaging for its low sensitivity to the motion-induced phase errors. However, EPI is prone to susceptibility changes at different tissue interfaces, which might demonstrate as diffuse hypo-intensity [33, 34]. The bleeding within the metastatic tumor increases the interface of the microarchitecture. Furthermore, the paramagnetic blood products itself results in the susceptibility artifact because of the variation of the magnetic homogeneity.

The variation of FA values measured within the metastatic tissue also confirms the sensitivity of DTI sequence to magnetic field inhomogeneity. Therefore, DTI images are more likely to show hemorrhage in metastatic tumors, thus increasing the sensitivity of detection.

The enhancing part of the tumor on post-contrast images showed slightly high signal on DTI, which was consistent with the pathological mechanism caused by the high cell density in the active area of tumor hyperplasia, which result in the focal diffusion constraint. Therefore, the presence of the high signal in the lesion area on the DTI could reflect

the tumor activity. This may provide a promising reference index for judging the therapeutic effect and prognosis.

There was no statistically significant difference in the FA value change rate between the adjacent and distant peritumoral edema of metastatic brain tumors. The reason is explained as follows:

1. histologically, brain metastases are similar to the primary tumor, with no blood–brain barrier but having extremely high capillary permeability;
2. high expression of VEGF in brain metastatic tumors generates immature neoplastic neovascularization with increased vascular permeability [31, 35];
3. the tumor compression on adjacent veins leads to simple vasogenic edema (the small foci with large edema and the large foci with small edema seen in the study might explain that some edema is caused by tumor compression of the surrounding blood vessels).

Therefore, the edema surrounding the metastasis is simple vasogenic edema without tumor cell infiltration. There are similar histological structures in the adjacent and distant peritumoral edema, resulting in no statistically differences in the change rate of FA value.

Regarding the detection rate of lesions, the number of lesions detected by DTI was fewer than post-contrast images. Reviewing the images from both sequences, the small (<7 mm in diameter) superficial metastatic brain tumors underneath the inner cranial plate could be documented on post-contrast MRI scans, but poorly on DTI. Such difference is likely due to DTI sequence's sensitivity to the magnetic field inhomogeneity. Furthermore, the enhanced MRI sequence used in this study is 3D T1WI, which provides more morphological details for small lesion characterization. Nevertheless, the consistency of the DTI and contrast-enhanced 3D T1WI scan is good.

A limitation of this study is the small sample size. Also, most of the subjects were patients with lung cancer, which has the predilection to hemorrhage. The treatment regime might induce the intratumoral hemorrhage. All these factors increased the sensitivity of the DTI to detect the lesion, thus resulting the bias. So, it should be further confirmed whether this advantage can be found for other brain metastases and patients who have not done antineoplastic therapy yet. Nevertheless, since in clinical practice most of the patients are diagnosed brain metastases in the follow-up and under long-standing chemotherapy, the situation of this study can still be representative, might provide reference to clinical practice.

In conclusion, DTI can detect much more brain metastatic tumor lesions than the conventional non-contrast MRI sequences, especially metastases with intratumoral hemorrhage. It can be an alternative and complementary scan protocol for the patient with contraindication to

contrast-enhanced MRI examination. At the same time, because DTI is more sensitive to the diffusivity of the water molecules, which in turn may be associated with the activity of the tumor, it might be used to determine the treatment efficacy and prognosis.

Acknowledgments This work was supported by the Department of Science and Technology of Guangdong Province [Applicable Grant or Contract Numbers: No. 2014A020212304].

Compliance with ethical standards

Conflict of interest All authors declare that there is no conflict of interest.

Ethical standards This article does not contain any studies with human participants or animals performed by any of the authors

Ethical approval The Ethic Committee approved this retrospective study.

Statement Magnevist is still used to be the routine contrast medium during MRI in China. There is no associated prohibition about the use of the Magnevist.

References

1. Owonikoko TK, Robin AM, Shim H et al (2014) Current approaches to the treatment of metastatic brain tumours. *Nat Rev Clin Oncol* 11:203–222
2. Menezes ME, Minn I, Sarkar D et al (2016) Detecting tumor metastases: the road to therapy starts here. *Adv Cancer Res* 132:1–44
3. Sze G, Heier L, Johnson C et al (1990) Detection of brain metastases: comparison of contrast-enhanced MR with unenhanced MR and enhanced CT. *AJNR Am J Neuroradiol* 11:785–791
4. Kaal EC, Taphoorn MJ, Vecht CJ (2005) Symptomatic management and imaging of brain metastases. *J Neurooncol* 75:15–20
5. Pope WB (2018) Brain metastases: neuroimaging. *Handb Clin Neurol* 149:89–112
6. Davis PC, Hoffman JC Jr, Hudgins PA et al (1991) Diagnosis of cerebral metastases: double-dose delayed CT versus contrast-enhanced MR imaging. *AJNR Am J Neuroradiol* 12:293–300
7. Ahn SJ, Chang JH, Chung TS et al (2014) The added value of double dose gadolinium enhanced 3D T2 fluid-attenuated inversion recovery for evaluating small brain metastases. *Yonsei Med J* 55:1231–1237
8. Bucci M, Berman JI, Berger MS et al (2013) Quantifying diffusion MRI tractography of the corticospinal tract in brain tumors with deterministic and probabilistic methods. *Neuroimage Clin* 3:361–368
9. Tsougos I, Theodorou K, Fezoulidis I et al (2012) Differentiation of glioblastoma multiforme from metastatic brain tumor using proton magnetic resonance spectroscopy, diffusion and perfusion metrics at 3T. *Cancer Imaging* 12:423–436
10. Masch WR, Tsien C, Wang PI et al (2016) Comparison of Diffusion tensor imaging and magnetic resonance perfusion imaging in differentiating recurrent brain neoplasm from radiation necrosis. *Acad Radiol* 23:569–576
11. Young RJ, Brennan N, Jenabi M et al (2017) Comparison of compressed sensing diffusion spectrum imaging and diffusion tensor

- Imaging in patients with intracranial masses. *Magn Reson Imaging* 36:24–31
12. O'Donnell LJ, Rigolo L, Suter Y et al (2016) Automated white matter fiber tract identification in patients with brain tumors. *Neuroimage Clin* 13:138–153
 13. Bette S, Boeckh-Behrens T, Gempt J et al (2017) Local fractional anisotropy is reduced in areas with Tumor recurrence in glioblastoma. *Radiology* 283:499–507
 14. Chaudhary N, Gemmete JJ, Gu Y et al (2015) Diffusion tensor imaging in hemorrhagic stroke. *Exp Neurol* 272:88–96
 15. Diedenhofen B, Musch J (2015) Cocor: a comprehensive solution for the statistical comparison of correlations. *PLoS ONE* 10(3):e0121945
 16. Ellingson BM, Erickson BJ, Smits M et al (2015) Consensus recommendations for a standardized brain tumor imaging protocol in clinical trials. *Neuro Oncol* 17:1188–1198
 17. Jeon JY, Moon WJ, Roh HG et al (2014) Effect of imaging time in the magnetic resonance detection of intracerebral metastases using single dose gadobutrol. *Korean J Radiol* 15:145–150
 18. Nagai A, Shibamoto Y, Hashizume C et al (2010) Increases in the number of brain metastases detected at frame-fixed, thin-slice MRI for gamma knife surgery planning. *Neuro Oncol* 12:1187–1192
 19. Gil B, Hwang EJ, Jang J et al (2016) Detection of leptomeningeal metastasis by contrast enhanced 3D T1-SPACE: comparison with 2D FLAIR and contrast-enhanced 2D T1-weighted images. *PLoS ONE* 11:e0163081
 20. Mayr NA, Muhonen MG, Nguyen HD et al (1994) Cost-effectiveness of high-dose MR contrast studies in the evaluation of brain metastases. *AJNR Am J Neuroradiol* 15:1053–1061
 21. Toth GB, Varallyay CG, Bashir MR et al (2017) Current and potential imaging applications of ferumoxytol for magnetic resonance imaging. *Kidney Int* 92:47–66
 22. Subedi KS, Saitoh J, Suzuki Y et al (2013) Usefulness of double dose contrast-enhanced magnetic resonance imaging for clear delineation of gross tumor volume in stereotactic radiotherapy treatment planning of metastatic brain tumors: a dose comparison study. *J Radiat Res* 54:135–139
 23. Kikuchi K, Obara M, Togao O et al (2015) 3D MR sequence capable of simultaneous image acquisitions with and without blood vessel suppression: utility in diagnosing brain metastases. *Eur Radiol* 25:901–910
 24. Villanueva-Meyer JE, Cha S, Mabray MC (2017) Current clinical brain tumor imaging. *Neurosurgery* 81:397–415
 25. Kuhnt D, Kapur T, Richter M et al (2013) Fiber tractography based on diffusion tensor imaging compared with high-angular-resolution diffusion imaging with compressed sensing: initial experience. *Neurosurgery* 72:165–175
 26. Hoy AR, Keckskemeti SR, Alexander AL (2015) Free water elimination diffusion tractography: a comparison with conventional and FLAIR DTI Acquisitions. *J Magn Reson Imaging* 42:1572–1581
 27. Richter M, Zolal A, Buchfelder M et al (2013) Evaluation of diffusion-tensor imaging-based global search and tractography for tumor surgery close to the language system. *PLoS ONE* 8:e50132
 28. Bette S, Wiestler B, Delbridge C, Huber T, Boeckh-Behrens T, Meyer B et al (2016) Discrimination of different brain metastases and primary CNS lymphomas using morphologic criteria and diffusion tensor imaging. *Fortschr Röntgenstr* 188:1134–1143
 29. Franchino F, Rudà R, Soffietti R (2018) Mechanisms and therapy for cancer metastasis to the brain. *Front Oncol* 8:161
 30. Caffo M, Caruso G, Cutugno M et al (2013) Innovative therapeutic strategies in the treatment of brain metastases. *Int J Mol Sci* 14:2135–2174
 31. Hanibuchi M, Kim SJ, Nishioka Y et al (2014) The molecular biology of lung cancer brain metastasis: an overview of current comprehensions and future perspectives. *J Med Invest* 61:241–253
 32. De Bock K, Carmeliet P, Cauwenberghs S (2011) Vessel abnormalization: another hallmark of cancer? Molecular mechanisms and therapeutic implications. *Curr Opin Genet Dev* 21:73–79
 33. Wu W, Miller KL (2017) Image formation in diffusion MRI: a review of recent technical developments. *J Magn Reson Imaging* 46:646–662
 34. Drake-Pérez M, Fitsiori A, Lovblad K et al (2018) Clinical applications of diffusion weighted imaging in neuroradiology. *Insights Imaging* 9:535–547
 35. Ji V, Zurita M, Oya S (2001) Expression and significance of vascular permeability factor in tumour infiltrating lymphocytes of brain metastases. *Acta Neurochir (Wien)* 143:153–157

Publisher's Note Springer Nature remains neutral with regard to jurisdictional claims in published maps and institutional affiliations.